

CONTRACT N°: RII3-CT-2004-506065

ISSUE CERTIFICATE

# EURONS



## EUROpean Nuclear Structure research

Activity **JRA09:RHIB**Identification: **D-J09-1.1**Revision: **0**

Final activity report 2008

Dissemination level: *PU*Issued by: *TUM*Reference: *EURONS-T-J09-1*Status: *Final***Summary:**

High-resolution tracking diamond detectors and their specific readout electronics have been developed, tested and implemented to the experimental setup at GSI cave-C.

	Roman Gernhäuser, TUM	Thomas Aumann GSI	
14.11.2008			
DATE	RESPONSIBLE Name/Company Signature	WP LEADER Name/Company Signature	COORDINATOR Name/Company Signature

# Integrated Infrastructure Initiative for European Nuclear Structure Research (EURONS)

## Joint Research Activity JRA09: Reactions with high-intensity beams of exotic nuclei (RHIB)

### Task T-J09-1: High-resolution tracking diamond detectors

#### Introduction

In most cases experiments using exotic beams have to include a twofold setup for identifying particles and their kinematical properties before and after the secondary reaction target. For the large variety of different experiments proposed for the R<sup>3</sup>B setup, various tracking-detector systems with different demands are required.

The incoming beam will be tracked at the dispersive focus of the FRS in order to determine beam momentum, angle and position of incidence on the target, and, similarly, for the spectrometer after the target. The velocities of the incoming beam as well as those of the fragments have to be determined with a resolution of  $\Delta\beta/\beta < 10^{-3}$  in order to achieve unique isotope identification. Using 140 m distance between the dispersive focus at the FRS and the reaction target at the R<sup>3</sup>B setup, the requirements for time-of-flight (TOF) detectors are quite moderate ( $\sigma_t < 100$  ps). Also a moderate position resolution of  $\Delta x = 3$  mm is sufficient. At the present FRS, heavy-ion rates rarely exceed  $10^5 - 10^6$  s<sup>-1</sup>. At the future Super-FRS, however, the detectors should be able to cope with heavy-ion rates of  $10^7$  to  $10^8$  s<sup>-1</sup> at the dispersive focus (FX) for quite exotic beams like e.g. <sup>132</sup>Sn.

For the high momentum-resolution mode ( $\Delta p/p < 10^{-4}$ ), however, needed for several experiments, the situation is quite different. The position resolution of all tracking devices has to be better than  $\Delta x < 0.5$  mm. Especially the vertex and angle reconstruction at the secondary target will need a much better resolution of  $\Delta x \sim 0.2$  mm. The angular scattering and momentum spread introduced by the tracking detectors in the target region have to be small compared to these numbers while the detectors inside the FRS and after the spectrometer could use a more massive layout. Also the expected background limits the material budget of the detectors in the target area.

The R<sup>3</sup>B project is a multi-purpose setup for very different branches of experiments. Therefore, the development of position-sensitive time-of-flight detectors with good resolution for tracking of exotic heavy ions is required, using minimum mass density to suppress efficiently parasitic reactions and multiple scattering. Development of such detectors based on diamond material has been supported by the EURONS FP6 program as Task T-J01. Results from the different sub-tasks and their deliverables are reported here.

### **Subtask T-J09-1.1: Investigations of current developments of diamond detectors**

Chemical-Vapor-Deposition (CVD) diamond is a detector material with fast signals, large charge carrier mobility, smallest lattice constant, and large band-gap [1][7d] resulting in radiation hardness, very good timing and high count-rate capability. These properties make it an ideal material for heavy-ion tracking and TOF detectors especially for the R<sup>3</sup>B experiment where a minimum material budget around the target is essential.

Properties of ideal single crystal diamonds (SCCVDD) are being investigated in the NoRHDia [2] collaboration. Currently, substrate material for SCCVDD is available only in small sizes ( $< 5 \times 5 \text{ mm}^2$ ) and in quantities which still rule out an application in most secondary-beam experiments which have to cope with large-area focal planes. Polycrystalline diamond material produced by chemical vapor deposition (PCCVDD) has been successfully used as a detector material at GSI for quite some years at several experiments (HADES, FOPI,...). It can be produced in layers of 10  $\mu\text{m}$  up to 1 mm and in wafer sizes up to 6 inch. Principle properties of the material and possible detector applications have been investigated by the RD42 collaboration [7a-d]. These results had to be verified for different material qualities from different providers as well as their extrapolation to the regime of heavy ions with a significantly higher specific energy loss. Most applications of this material currently aim for beam and radiation monitoring or time-of-flight measurements of monolithic detectors. We carried on this development towards highly segmented, thin, large area ( $25 \times 25 \text{ mm}^2$ ) devices.

Systematic investigations have been made with material from two different suppliers, the "IAF" Fraunhofer Institute Freiburg and their associated company "Diamond Materials", and "Element6" (E6) later called "Diamond Detectors". These are currently the only European commercial providers for detector-grade PCCVDD. We have produced small test detectors of  $10 \times 10 \text{ mm}^2$  area with different thicknesses ranging from 20  $\mu\text{m}$  up to 300  $\mu\text{m}$ . Segmentation into four strips in x and y direction on the front and the back side each was done by vapor deposition of different metallic layers (Al, Ti/Au, Cr/Au) using a passive shadowing mask made of 50  $\mu\text{m}$  tungsten wires.

A variety of tests was performed at the Munich Tandem accelerator using <sup>16</sup>O and <sup>7</sup>Li beams of 117 MeV and 48 MeV, respectively. The detectors were set up as a stack consisting of a diamond detector and a Si diode. After passing through the diamond detector the beam was stopped in the diode which provided a trigger and the residual-energy signal. To achieve nearly saturated drift velocities, for most of the measurements reported here we applied a field of 2 V/ $\mu\text{m}$ .

## Tests of Material Properties

In polycrystalline CVD-diamond material the electrons and holes only drift a fraction of the thickness in the electric field and recombine preferentially at the grain boundaries. This charge collection capability typically reduces the signal amplitude but also widens the energy distribution (see fig. 1). Using the Li beam an average collected charge of 25 fC corresponding to a charge collection depth of 12  $\mu\text{m}$  was found [3] in 50  $\mu\text{m}$  thick detectors made from IAF material. This is already sufficient for heavy-ion detection. A nearly linear increase of these numbers has been observed for larger material thicknesses. It turned out that the material from E6 provides on average a 30% larger charge collection depth. But due to the large energy loss of heavy ions this is not a very critical quantity.

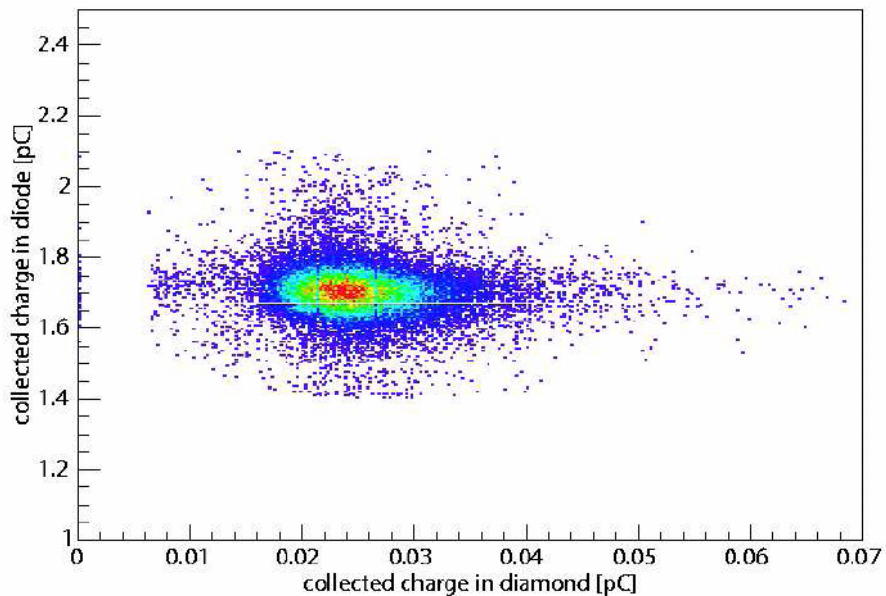


Fig. 1: Collected charges in a stack of a 50  $\mu\text{m}$  diamond detector and a 500  $\mu\text{m}$  silicon diode.

In the same type of measurements also the detection efficiency was determined. Using the Li beam and an energy cut of 20 % of the average signal, 98 % of all particles passing a 50  $\mu\text{m}$  thick diamond are recognized (see figure 1). This value is consistent with the segmentation gaps of 50  $\mu\text{m}$  at a pitch of 2 mm. These results have been confirmed by measurements in the HADES Experiment (see below) where some of our samples had been used as in-beam detectors [4]. So the question was raised how the efficiency between the metallized areas drops. This is discussed in the following section.

Radiation hardness is one of the key issues of diamond detectors. It was tested on the same type of 4-fold segmented detectors using a 117MeV  $^{16}\text{O}$  beam which is available with very high intensities. As its specific energy loss is very similar to that of the heaviest ions provided at GSI energies, these tests were assumed to be as close as possible to a realistic scenario in a radioactive-beam facility. In a 100  $\mu\text{m}$  detector made of IAF material, the average signal amplitude linearly dropped to about 70 % [5a] with increasing dose up to a dose of  $10^{11}$   $^{16}\text{O}$  ions per  $\text{mm}^2$ . This would roughly correspond e.g. to a full-time operation of 1 year at the focal plane of the planned Super FRS.

## TOF measurement

Fast signals are one of the outstanding features of diamond. To test the TOF performance of our thin diamond detectors for heavy ions, two of our test detectors have been implemented in the HADES experiment beam-line as a start and a veto detector for the HADES trigger. The new start detector was made from a 50  $\mu\text{m}$  substrate

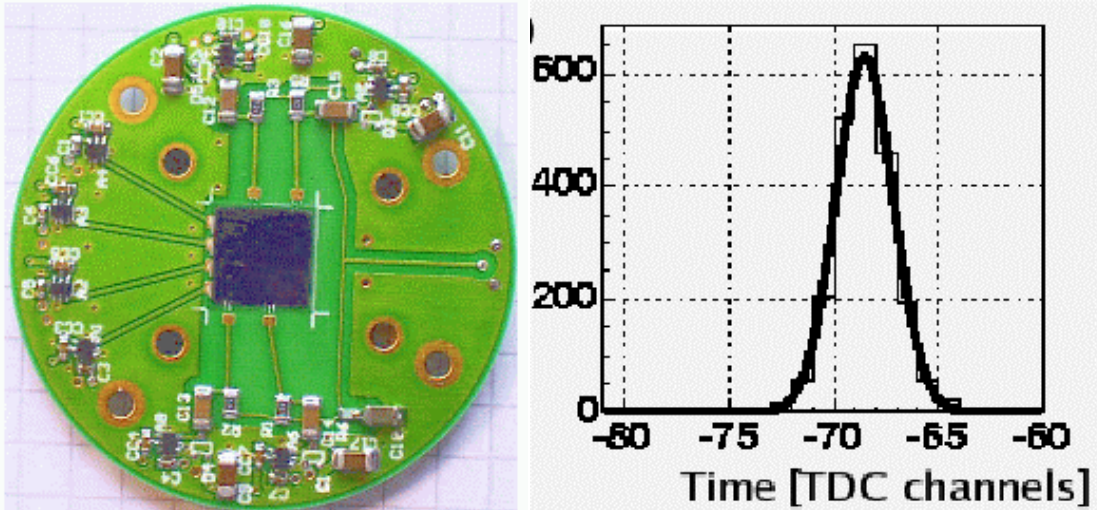


Figure 2: 10 x 10 mm diamond detector with on-board preamplifier tested in the HADES experiment (left). A time resolution of  $\sigma_{\tau} \sim 60$  ps was achieved (right).

material from IAF. The segmentation is four strips in x direction and four strips in y direction. It is mounted on a newly developed circuit board which is based on fast, low-noise, low power, 2 GHz broad-band current preamplifiers as a first stage (see Fig. 2) with a gain of 10. In a second stage the signals are amplified by single-channel amplifiers developed at GSI (DBA-II [10]) with a gain of 130. The veto detector segmented and operated in the same way was made of 100  $\mu\text{m}$  IAF material. For the experiments a  $^{40}\text{Ca}$  beam of 1.9 A GeV was used with an intensity of up to  $2 \times 10^6 \text{ s}^{-1}$ .

From the time of flight between the two detectors a resolution of  $\sigma_{\tau} \sim 60$  ps (see Fig. 2) for each individual detector was found. This did not significantly depend on the signal amplitude. From the signal rise-time and noise figures, a two times better time resolution was expected. Reasons for this are not clear up to now and have to be investigated in further tests.

## Detector operation and leakage current

After production, without exposure to radiation, leakage currents of typically  $5 \text{ nA/cm}^2$  are rather constant up to fields of  $5 \text{ V}/\mu\text{m}$  and increase by a factor of 10 between 5 and  $7 \text{ V}/\mu\text{m}$ . There was no significant difference observed for operation in air, gas or vacuum. To achieve nearly saturated drift velocities, for most of the measurements reported here we applied a field of  $2 \text{ V}/\mu\text{m}$ .

During irradiation in some cases the situation changed completely, and different effects have been observed. Especially for some samples where the surfaces had been treated by plasma etching or heat treatment, the leakage current ruled out any further use.

Basically there are 4 components which show up in the resistance of the material:

- 1) The basic leakage current (blc) described before which is usually quite small and constant. Only samples exposed to a quite crude treatment or from bad production batches have a  $\text{blc} > 50 \text{ nA/cm}^2$ .
- 2) The typical blc increases after large exposure to radiation, typically by  $100 \text{ nA}$  per  $10^{12} \text{ ions/cm}^2$ .
- 3) There is an additional beam-induced current which is typically a factor of 10 higher than what is expected due to energy loss inside the material.
- 4) Persistent particle-induced currents (PPC) which behave very similar to what is discussed in the literature as persistent photo currents [1]. The PPC builds up during exposure to radiation over a time of many minutes and sometimes reaches values of  $20 \mu\text{A}$ . After switching off the radiation, it also decays with large time constants in the order of minutes.

Especially for the material from IAF we saw the different components varying by more than one order of magnitude without change of any of the production parameters.

Even samples from different areas of the same diamond wafer behave significantly different. On the other side, it was observed that once a sample showed a significant increase of one of the four components, this was never cured by any post-treatment steps after reprocessing the surfaces. So our conclusion was that these effects seem to originate from the production procedure where we have only a very limited influence on. In case of the samples from E6 we had observed very good properties for samples we got already in 2005 and 2006. Unfortunately, the quality of the material we got in 2007 was less promising and a significant increase of the PPC was observed.

In conclusion, the PPC is the most severe problem which delayed the development of the full-size prototypes by more than 2 years. Together with IAF we made many iterations of changes in the production process like changing substrate temperatures, gas composition, growth speed, surface polishing, surface treatment with oxygen plasma or plasma etching, heat treatment, and different chemical etching procedures. There were no systematic improvements observed, and only 30% of the material is produced with leakage current levels within the specifications.

## Subtask T-J09-1.2: Prototype detector developments and tests

### Segmentation of the detectors

For the development of highly segmented detectors made of a non homogenous material, especially the performance at the segment boundaries is of fundamental interest. To determine the influence of the segmentation on the overall detection efficiency, we produced test detectors of  $10 \times 10 \text{ mm}^2$  from polycrystalline CVD diamond. The Al metallization is 64 strips on the front side, i.e. a strip width of  $110 \text{ }\mu\text{m}$  and a gap between two strips of  $30 \text{ }\mu\text{m}$ , and 4 strips of  $2 \text{ mm}$  width and a gap of  $50 \text{ }\mu\text{m}$  on the back side. For investigation of spatial charge-collection efficiencies we tested different detector samples with the Munich micro beam facility using the superconducting nanoscope for applied nuclear physics – SNAKE [5].

The diamonds have been scanned with a step size down to  $2 \text{ }\mu\text{m}$  in  $x$  and  $3 \text{ }\mu\text{m}$  in  $y$  direction which roughly correspond to the size of the beam spot. Using again a  $48 \text{ MeV}$  Li beam, signal amplitudes for each individual strip on the detector were recorded.

Figure 3 shows such a signal map across the strip boarder of the fourfold side of a  $50 \text{ }\mu\text{m}$  thick diamond from IAF. Clearly, the signal amplitudes on average drop in the  $50 \text{ }\mu\text{m}$  gap between two  $2 \text{ mm}$  wide strips. The  $y$ -projection shows a less efficient area with a width of  $40 \text{ }\mu\text{m}$  at the segmentation line. For a  $30 \text{ }\mu\text{m}$  gap, the area of reduced amplitudes was measured to be  $15\text{-}20 \text{ }\mu\text{m}$  wide. While in the  $50 \text{ }\mu\text{m}$  detectors the inefficient areas are  $10 \text{ }\mu\text{m}$  more narrow than the gap size, this number is  $20 \text{ }\mu\text{m}$  in case of  $100\text{ }\mu\text{m}$  thick detectors. Using segmentation gaps of  $10 \text{ }\mu\text{m}$  and  $20 \text{ }\mu\text{m}$ , respectively, we expect full efficiency over the entire area. This observation is also consistent with the average grain size of  $10\text{-}20 \text{ }\mu\text{m}$  in diameter in the poly-crystalline material we used. More details for these measurements are reported in [5].

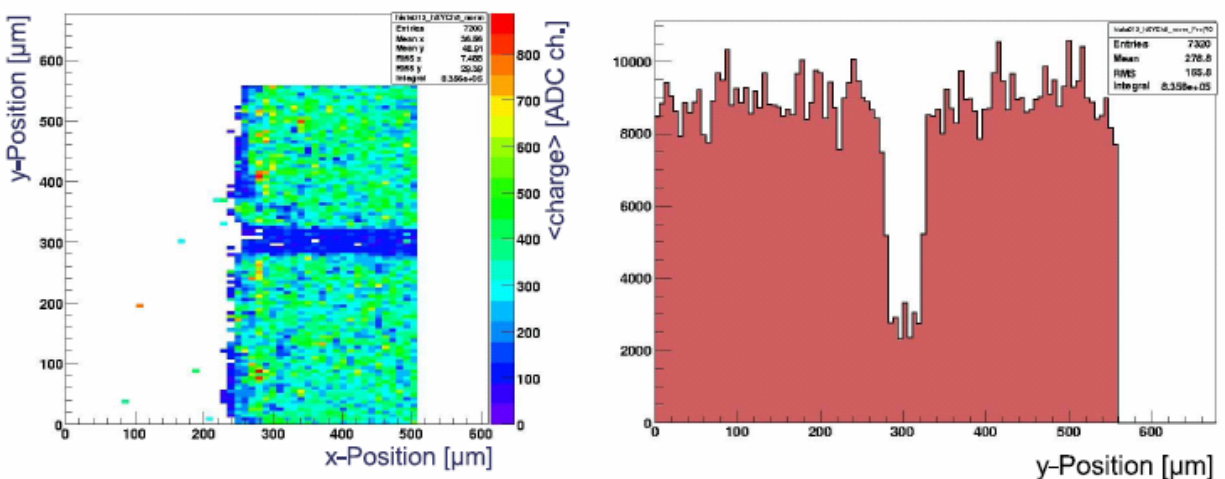


Fig.3: Two-dimensional amplitude scan of a  $50 \text{ }\mu\text{m}$  segmentation gap (left), and its  $y$ -projection (right).

## Large-area prototype detector production

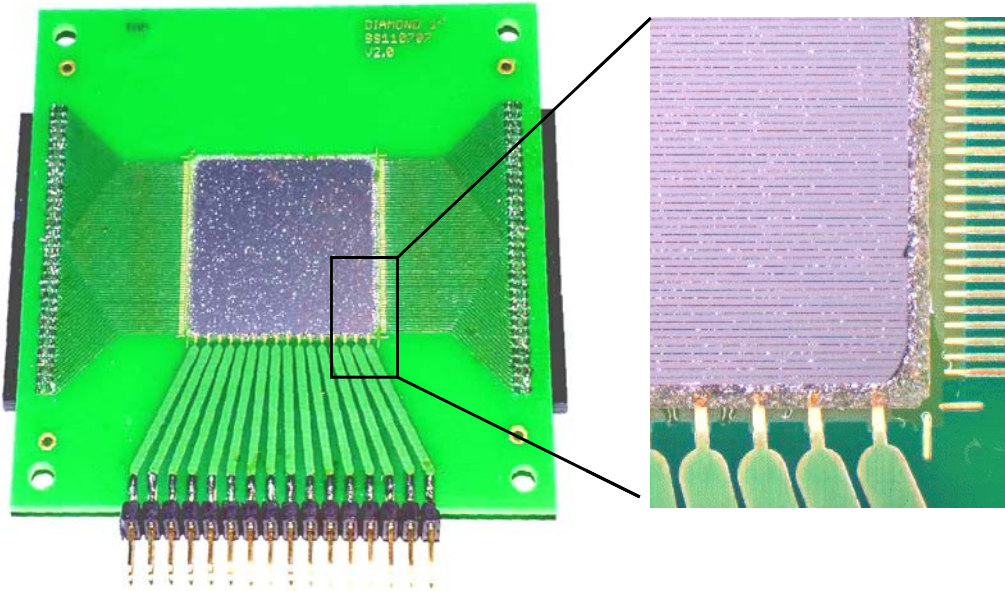


Figure 4: Layout of a large-area prototype detector mounted on a test PCB.

In order to avoid additional mechanical problems for the larger-area prototypes ( $25.4 \times 25.4 \text{ mm}^2$ ), the  $100 \mu\text{m}$  thick substrate material was chosen. The side used for position measurements is segmented into 128 strips with a pitch of  $190 \mu\text{m}$  and gaps of  $20 \mu\text{m}$ . This has been done by metallization with aluminum and lithographic methods. The back side is used for TOF measurements. It is divided in 16 aluminum strips perpendicular to the front side strips with gaps of  $50 \mu\text{m}$  in between. The resulting 3% of efficiency loss could not be avoided as this is the unpolished growth side of the material where lithographic methods cannot be applied due to the surface roughness. Figure 4 shows the details of such a device already mounted on a PCB board with the appropriate connectors for all of the 144 channels. The production is a rather time-consuming multi-step process. First the substrate material has to be cleaned and the diamond surface has to be finished with oxygen to avoid surface conductivity. For this we used a mixture of 2/3 sulfuric acid and 1/3 hydrogen peroxide. After rinsing and drying for 1 hour at  $150 \text{ C}^\circ$ , the polished side of the material was covered with a  $800 \text{ nm}$  aluminum layer by thermal vapor deposition at room temperature. After covering it with  $1 \mu\text{m}$  of photo resist by spin coating, this was structured by UV-light exposure through a glass mask in direct contact. After several steps of chemical processing and etching, the  $170 \mu\text{m}$  wide metallization strips are nicely separated. Since we found no way to cut the diamond substrate after metallization without getting conductivity at the edges, a significant fraction of the technological development was spent learning to work with square-shaped final-size material. Special difficulties involve avoiding edge effects during spin coating, mask alignment, etching times, and also avoiding shorts between the strips at edges and corners with having only a  $500 \mu\text{m}$  wide passive ring around the active area. There is still work in progress to reduce this distance further down to  $200 \mu\text{m}$ . The 16

back-side strips are directly produced by aluminum vapor deposition through a shadowing grid made of 50  $\mu\text{m}$  tungsten wires directly placed in front of the unpolished growth side of the material. In a final step, the whole detector is baked at 300 C° for several hours to provide a better adhesion of the aluminum layers. Four of these detectors have been produced and mounted on test PCB boards. Like in the case of silicon detectors, the contacts of the 1.6 mm wide back-side strips have been realized with a conductive glue while the front-side contacts are performed with wire bonding.

## Development of readout electronics

Concerning the readout of PCCVD diamond detectors, the special properties of the material have to be taken into account. The composition of many small crystal grains and the short lifetime of the charge carriers inside the material do not allow a large spread of signal between neighboring segments. The large spread of signal amplitudes requires a large dynamic range of the electronics, while the amplitude resolution is a minor issue which is required only for walk correction in the TOF measurements. On the other hand, the fast rise time of the signals in the order of a few hundred ps requires a careful design of impedances to avoid reflections. Our new readout concept is based on a digital single-strip readout for the highly-segmented side to obtain the position information in one dimension, and on fast analog signal transport to conventional discriminators to obtain TOF and a rough position information in the other dimension. For readout of the highly segmented front sides of the detectors, a new front-end board was built based on the APV25 chip developed at CERN for the CMS experiment. The board shown in Fig. 5 includes already a capacitive coupling to the detector, protection circuitry, digital addressing of the boards, a special pitch adapter, and one APV25 chip each.

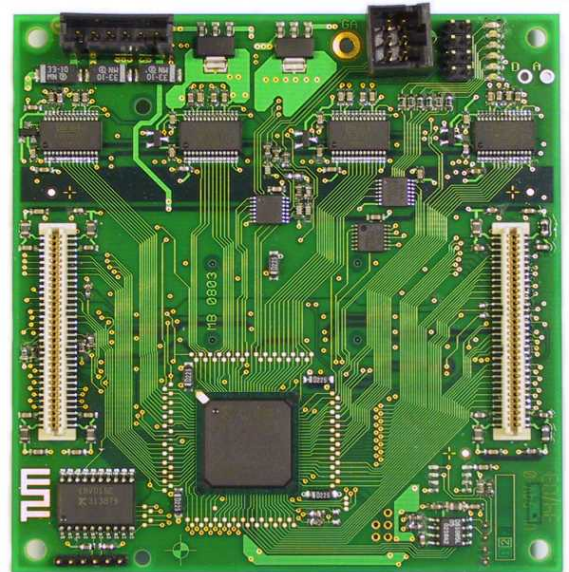


Figure 5: New APV-front-end board for 128 channels (left); GTB bridge board with 4 ADCs to connect 4 of the front-end boards to the digital GTB bus (right).

The APV25 [9] is a 128-channel analog chip developed for Silicon strip detectors with preamplifier, shaper, and 192 columns of analog storage. The fast shaping time of 50 ns and the included analog daisy chains for each of the 128 channels per chip nicely fits to the planned NUSTAR readout scheme.

As an important milestone, the combination of ultra-fast diamond signals and front-end electronics designed for silicon-detector readout was tested. Although the signal range of 8 mip (800 ke) seems to be quite small for heavy ions, we measured a position resolution of one strip (see Fig. 6) even for a Xe beam, without any attenuation in the APV (see also [8]). Nevertheless, in this case many neighboring strips showed signals out of range, and we had to calculate positions by the center-of-gravity method. To reduce the amount of data and to simplify the method, we also tested capacitive attenuators which reduced the signal amplitude by up to a factor of 10 without increasing the noise above 2500 electrons. As the bigger part of the signal is fed to ground directly at the detector in this case, we expect a much better performance of the timing readout at the opposite side of the detector. This is a matter still to be tested.

Four of the APV25 front-end boards (512 channels in total) were read out by a GTB Bridge Board (GTB3) [6]. This board was originally developed for R<sup>3</sup>B to read out other front-end boards based on the GASSIPLEX chip. The GTB3 (see Fig. 5) consists of four 12-bit ADCs with gain and offset stages and a large FPGA for control logic and data handling. It provides zero suppression, offset subtraction, and the GTB-bus interface. A full implementation of the APV25 readout was possible by only changing smaller parts of the VHDL code for the FPGA without changing the hardware. Using a SAM3 VME module for data collection and a typical occupancy of 10 strips per detector, a total dead

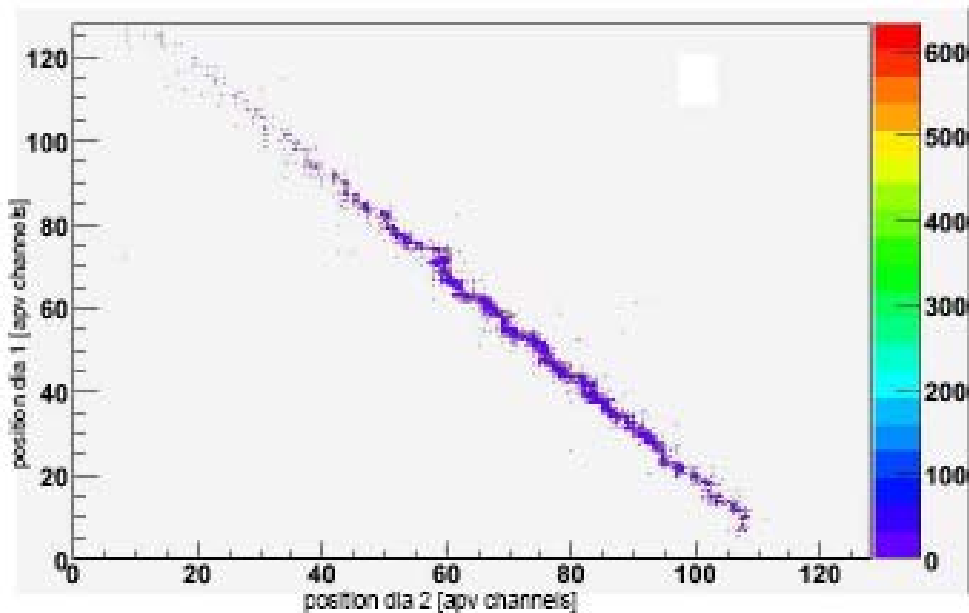


Figure 6: Position correlation of two diamond strip detectors [200  $\mu$ m].

time of 100  $\mu$ s was achieved in single-event readout mode. Currently a new version of the GTB3 with multi-event buffering and time stamping is developed which will make use

of the 32-event analog buffering inside the APV25 to allow a quasi dead-time-free readout.

## Full system tests

Two independent full-system tests have been performed in 2007 and 2008. The first one [8] used a  $^{129}\text{Xe}$  beam of 600 A MeV with an intensity of  $10^5 \text{ s}^{-1}$ . A compact stack of two detectors of  $25.4 \times 25.4 \text{ mm}^2$  size was mounted in air at the FRS middle focus to measure particle positions with respect to each other. Each detector was read out by two APV chips. Figure 6 shows the position correlation of particles in the two detectors. The intrinsic resolution is in the order of  $200 \mu\text{m}$ . The additional structures shown are caused by signal coupling of non-neighboring channels due to operation far off the dynamic range of the APV.

In a second test we used a similar, close to full scale,  $\text{R}^3\text{B}$  target tracking device. It was included in the full  $\text{R}^3\text{B}$  prototype detector-setup and read-out system in cave C at GSI. The measurements were performed in a series of tests for the upcoming S327 experiment, using a  $^{12}\text{C}$  beam of about 1 A GeV. In this case, the energy loss is about two orders of magnitude lower than that of the Xe beam. Here, a typical strip multiplicity of 1 was observed with signal amplitudes covering half of the APV range but still nicely separated from noise. So the assumption of a position resolution of  $\Delta x < 200 \mu\text{m}$  should be clearly fulfilled. Due to their small signals, the 16 strips from the rear side of the detectors were read out with conventional integrating front-end electronics, timing filter amplifiers, and leading-edge discriminators; the signals were fed into a TDC using an in-beam scintillator as a time reference. Due to the poor performance of this electronics, we could only determine an upper limit of  $\sigma_t < 250 \text{ ps}$  for the time resolution in this case.

## Summary and deliverables

During the period of this project about 100 small-size test samples and several close to full-size micro strip PCCVD diamond detectors have been fabricated, mounted and tested. The production technique is well under control even for very thin  $50\mu\text{m}$  material. The detector tests presented have demonstrated the successful operation of medium-sized micro-strip diamond detectors for heavy ions. The successful operation of the complete tracking device was proven, as well as the expected position resolution, using a complete set of novel electronics also developed within the framework of this project. We have verified radiation hardness, good efficiency, and superior TOF resolution for various samples of the detectors which fulfill the requirements. In the electronics development a newly designed readout scheme including the highly integrated APV25 chip was implemented and tested, as well as novel fast broad-band preamplifiers.

Current work is focused on simultaneous TOF and position readout. Presently, the time resolution in the TOF branch suffers from digital and analog noise and crosstalk from the APV readout. It turned out that, in the full setup, the use of large band-width preamplifiers is limited to a gain of 50 which is not sufficient for very light ions. Also due

to signal transport on board and after the first stage, the gain in noise to rise time is negative when increasing the bandwidth to more than 1 GHz. In a revised version of the fast preamps we will therefore use a short integration time of 1 ns to improve the S/N ratio and make the whole operation of the fast signal readout more stable.

In the detector production, all the lithographic steps, mounting and handling procedures are well under control also for large-area samples down to a thickness of 100  $\mu\text{m}$ . We continue working together with both producers of the raw material to obtain a more reliable and constant material quality for large-area samples. At present, the reasons for the unpredictable behavior of the leakage currents are not fully identified and make cost estimates for future applications quite difficult. This problem had also produced the reported delays with respect to the work plan. Based on the work reported here, a full-scale detector setup for R<sup>3</sup>B (and later the Super FRS at FAIR) was funded by the German government and will be finished in 2009.

Our PhD Student Sabine Schwertel worked for 36 month full time on the project and will finish her thesis in 2008. Michael Böhmer spent 12 month (fte) on the development of the readout electronics, Sonja Winkler spent 18 month (fte) in the detector production and Roman Gernhäuser spent 12 month (fte) in experimental testing and coordination of the project. To allow for the excessive experimental testing in various places, there were additional contributions of about 6 months (fte) from other scientific staff of TU-München. All results and the individual steps reported here have been published in various reports [3][4][5][6][8] and in oral presentation at the R<sup>3</sup>B Collaboration meetings.

## Literature:

- [1] C. Nebel, *Semicond. Sci. Technol.* 18 No 3 (March 2003) S1-S11, PII: S0268-1242(03)58317-1
- [2] <http://www-norhdia.gsi.de/>
- [3] S. Schwertel et al., *GSI Scientific Report 2005 (GSI Report 2006-1)* 46.
- [4] S. Schwertel et al., *DPG spring meeting (2006)* HK21.78
- [5] S. Schwertel et al., *MLL Annual report (2006)*, 83
- [5a] S. Schwertel et al., *MLL Annual report (2005)*, 86
- [6] M. Böhmer, *TU-München, PhD Thesis (2006)*,  
<http://nbn-resolving.de/urn/resolver.pl?urn:nbn:de:bvb:91-diss20061006-1757209305>
- [7] The RD42 Collaboration, *Status Report 1999, CERN/LHCC 2000-011*,
- [7a] The RD42 Collaboration, *Status Report 1999, CERN/LHCC 2000-015*,
- [7b] W. Adam et al., *CERN-EP-2000-115*, Geneva, CERN, 24 Aug 2000
- [7c] W. Adam et al., *Nuclear Instruments and Methods A*, vol. A447, (2000), 244.
- [7d] W. Adam et al., *NIM A* 514 (2003) 79–86
- [8] S. Schwertel et al., *GSI Scientific Report 2007 (GSI Report 2008-1)* 216.
- [9] M. Raymond et al., *IEEE Conf. Rec (2000)*, 2, 113, ISBN: 0-7803-6503-8
- [10] P. Moritz et al., *8th Beam Instr. Workshop, AIP Proc. 451*, Stanford CA (1998)